Chemical signatures of Melaleuca quinquenervia leaves as precipitation proxies

Thesis submitted in accordance with the requirements of the University of Adelaide for an Honours Degree in Geology

Jake William Andrae

November 2014

THE UNIVERSITY of ADELAIDE

CHEMICAL SIGNATURES OF MELALEUCA QUINQUENERVIA LEAVES AS PRECIPITATION PROXIES

MELALEUCA LEAVES AS PRECIPITATION PROXIES

ABSTRACT

The eastern coast of Australia is susceptible to variations caused by the El Niño-Southern Oscillation. The geological record in this region is therefore ideal for studying the history of El Niño variability. However, site-specific proxies for precipitation amounts are needed to examine El Niño in the geologic past.
Carbon isotope ratios of leaves and the average chain length of leaf-wax *n*-alkanes have the potential to act as proxies for past rainfall. Carbon isotope ratios respond to changes in water availability (Stewart *et al*. 1995; Korol *et al.* 1999; Cornic 2000; Van de Water *et al.* 2002). Average chain length of leaf wax *n*-alkanes has also been found to relate to climatic variables, including temperature, humidity and water availability (Tipple & Pagani 2013; F. McInerney pers. comm. 2014).
These two measures are used in this study to develop proxies for climate in modern *Melaleuca quinquenervia* leaves. We hypothesised that leaves in drier environments would have smaller discrimination values than wetter environments. We also hypothesised that average chain length of leaf wax *n*-alkanes in modern *Melaleuca quinquenervia* will show longer chain length distributions at drier sites.
The discrimination of modern leaves is positively correlated with precipitation and precipitation-evaporation for the previous four years at each site, and statistically significant negative linear correlations of average chain length with precipitation and precipitation-evaporation exist. The correlations have significance as modern calibrations for palaeoclimate proxies.
These calibrations have important geological applications to lake sediments preserving sub-fossil leaves of *Melaleuca quinquenervia,* including a known site at Swallow Lagoon on North Stradbroke Island and other identified sites of potential sub-fossil leaf preservation. The calibrations developed in this study have the potential to help quantify past precipitation and El Niño variation across the east coast of Australia.

KEYWORDS

Geochemistry, stable carbon isotopes, average chain length, Melaleuca quinquenervia, precipitation, proxies, palaeoclimate

TABLE OF CONTENTS

LIST OF FIGURES

LIST OF TABLES

INTRODUCTION

Throughout Earth's history, climate has undergone considerable variation, and has been the result of, and cause of, many different changes in the state of the Earth. Understanding how and why the climate has varied is a significant area of research among the Earth science and Ecology fraternities, across many different geologic periods. Paleoclimatology is the study of climatic conditions in the past, achieved by examining geological records and applying proxies derived from the modern Earth to understand what these records potentially represent (Robinson & Dowsett 2010; Castañeda & Schouten 2011). Climate studies, whether they are focussed on the past or a modern context, produce data that can be used to help postulate what may happen to the climate in the future.

Precipitation in the geologic past is an important aspect of terrestrial climate that is often more difficult to reconstruct than temperature. The study of past precipitation is particularly important for understanding the behaviour of the El Niño-Southern Oscillation (ENSO) in the recent geologic past. ENSO is a meteorological phenomenon that affects the Pacific Region, including Australia and South America. On the east coast of Australia, El Niño events result in locally dry conditions, while La Niña events culminate in locally much wetter climatic conditions (Donders *et al*. 2007). Variations in precipitation influence plant characteristics, and as such, plants have the ability to record changes in this aspect of climate. The signature of stable isotopes within plant tissue and the molecular composition of plant components can be used to quantify environmental changes, both for the recent and the geologic past (Marshall *et al*. 2007; Eglinton and Eglinton 2008; Casteñada & Schouten 2011).

Carbon isotopes are particularly useful for these types of studies, due to their high abundance, simplicity in analysis, and because carbon isotope ratios vary with changes in photosynthetic assimilation of carbon. Two stable isotopes of carbon; ^{12}C and ^{13}C, are present in the Earth's atmosphere, as a component of molecules of CO_2. In plants, less ^{13}C is present in their tissues than what is in atmospheric CO_2, due to ^{12}C being favoured when CO_2 is taken up during photosynthesis (Farquhar *et al*. 1989a).
CO_2 diffuses from the atmosphere into the leaf through the stomatal pores, with some fractionation occurring against ^{13}C due to differences in velocity between the isotopes. In the most widely used photosynthetic pathway, C_3, a carboxylating enzyme, ribulose biphosphate carboxylase/oxygenase (rubisco), then acts on the CO_2 that has entered the leaf, discriminating against ^{13}C isotopes further (Marshall *et al*. 2007).

Variations in isotope fractionation can occur when a C_3 plant is exposed to greater water stress, such as a time when precipitation is low. Under dry conditions, stomatal conductance (flux of gases into and out of the leaf) in plant leaves decreases to minimize water vapour flux out of the leaf (Stewart *et al*. 1995; Korol *et al*. 1999; Cornic 2000; Van de Water *et al*. 2002). The model developed to explain carbon fractionation is given in the following formula (Farquhar *et al*. 1989b; Cernusak *et al*. 2013):

$$\Delta = a + (b - a)\, c_i/c_a \qquad (1)$$

Where Δ is carbon isotope discrimination, *a* is diffusional fractionation across the stomatal boundary (4.4‰), *b* is carboxylation fractionation (27‰), and c_i/c_a is the ratio of intercellular to ambient CO_2 concentrations.

When water resources are plentiful, stomata are open and the ratio of c_i/c_a increases towards a value of one. This means the plant has an almost infinite pool of atmospheric carbon dioxide, with both ^{12}C and ^{13}C isotopes to utilise. As c_i/c_a approaches a value of one, fractionation discrimination is closer to the value of *b*: 27‰. As stomatal conductance decreases to prevent water loss from the plant during times of stress, the ratio of c_i/c_a becomes smaller and approaches zero, where fractionation discrimination decreases towards the value of *a*: 4.4‰. When stomatal conductance is lower, carboxylation fractionation is dominant, ^{13}C is not as easily discriminated against due to a finite pool of isotopes to use and more ^{13}C must be utilised (Farquhar *et al*. 1989b). Studies have identified a negative linear correlation between mean annual precipitation (MAP) and bulk carbon isotope composition ($\delta^{13}C$) of C_3 plants (Stewart *et al*. 1995; Diefendorf *et al*. 2010; Prentice *et al*. 2010). Bulk carbon isotopic composition is calculated using Formula 2 (after Farquhar *et al*. 1982):

$$\delta^{13}C\ (‰) = (R_{sample} / R_{standard} - 1) \times 1000 \qquad (2)$$

Where R is the carbon isotope ratio of $^{13}C/^{12}C$; sample is the material being measured and standard is the Pee Dee Belemnite. The value obtained for $\delta^{13}C$ is reported in per mil (‰).

This correlation can also be viewed in terms of carbon isotope discrimination (Δ) (after Arens *et al*. 2000):

$$\Delta\ (‰) = (\delta^{13}C_{atmosphere} - \delta^{13}C_{plant}) / (1 + \delta^{13}C_{plant}/1000) \quad (3)$$

Where $\delta^{13}C_{atmosphere}$ is the atmospheric carbon isotope composition, with a modern average of approximately -8‰ (Cuntz 2011), and $\delta^{13}C_{plant}$ is the carbon isotopic composition of the plant material being measured. An increase in MAP results in a larger Δ between bulk leaf and atmospheric carbon isotope ratios, which corresponds to more negative $\delta^{13}C$ values.

Measured $\delta^{13}C$, and Δ derived from this can therefore be related to a plant's response to water stress. These values can not only be measured from modern plant tissue, but can be measured from preserved plant material, thus having the potential to quantify stored information about past climate when the right calibration is applied.

Similarly, leaf wax *n*-alkanes can be measured from the geologic past. Leaves utilise long chain leaf wax *n*-alkanes as an interface for protection against external environmental factors, and to assist in preventing water loss through evaporation (Jetter *et al*. 2006; Dominguez *et al*. 2010; Bush & McInerney 2013). Long chain *n*-alkanes are deemed to range from *n*-C21 to *n*-C37, and show an odd over even predominance (Bush & McInerney 2013). It has been theorised that in more extreme environments, such as environments with greater aridity, a greater number of long-chain *n*-alkanes that are more adept at protecting plants and preventing water loss are produced than shorter

chain lengths (Dominguez *et al*. 2010; Bush & McInerney 2013). Distributions of these *n*-alkanes that are found on leaf surfaces and preserved in soils have also been found to relate to climate variables, with average chain length (ACL) used to quantify these distributions.

A number of studies have reported temperature, humidity and water availability as major factors influencing ACL, and the production of leaf wax *n*-alkanes in general (Dodd & Poveda 2003; Hoffman *et al.* 2013; Tipple & Pagani 2013; Carr *et al.* 2014; F. McInerney pers. comm. 2014). A study looking in part at the effect of climatic variables on the ACL of *n*-alkanes found in Eucalypt and Acacia species found a significant correlation between ACL and variables including relative humidity, mean annual precipitation and aridity index. It deemed that evapotranspiration and water availability were major drivers for leaf wax *n*-alkane chain length distributions (Hoffman *et al*. 2013). Leaf wax *n*-alkane ACL may provide a significant proxy for climate.

This study proposes to quantify a correlation between climate variables, notably precipitation, for both Δ and ACL of *Melaleuca quinquenervia* leaves in a modern environment. The aim of this study is accomplished by sampling leaves of *Melaleuca quinquenervia* across a significant spatial precipitation gradient in the Brisbane and North Stradbroke Island region, and measuring the $\delta^{13}C$ and ACL of those leaves. By utilising one species, it is possible to eliminate other factors that contribute to variations in the carbon isotope compositions and ACL of leaves, such as plant functional type and photosynthetic pathway. The Δ and ACL values for trees on this spatial gradient are then analysed in the context of precipitation information available from present day

climate datasets, in order to develop a calibration that can be used to reconstruct precipitation.

We hypothesise that modern leaves will vary in their Δ values, with a drier environment being expressed by a smaller value of Δ, and a wetter environment by a larger Δ. We hypothesise that ACL in modern Melaleuca quinquenervia will vary depending on the amount of precipitation, with a larger average chain length for drier conditions. Calibrations of both carbon isotope discrimination and average chain length values in the context of their correlations with precipitation are valuable for their use as palaeoclimate proxies. The motivation for this study and its use of the species *Melaleuca quinquenervia* for the development of climate proxies stems from the discovery of sub-fossil preservation of leaves of this species in a core from the bed of Swallow Lagoon, North Stradbroke Island, spanning ~7000 years (C. Barr & J. Tibby pers. comm. 2014). A number of similar sites throughout Queensland with potential for sub-fossil leaf preservation of this species have been determined (Figure 1).

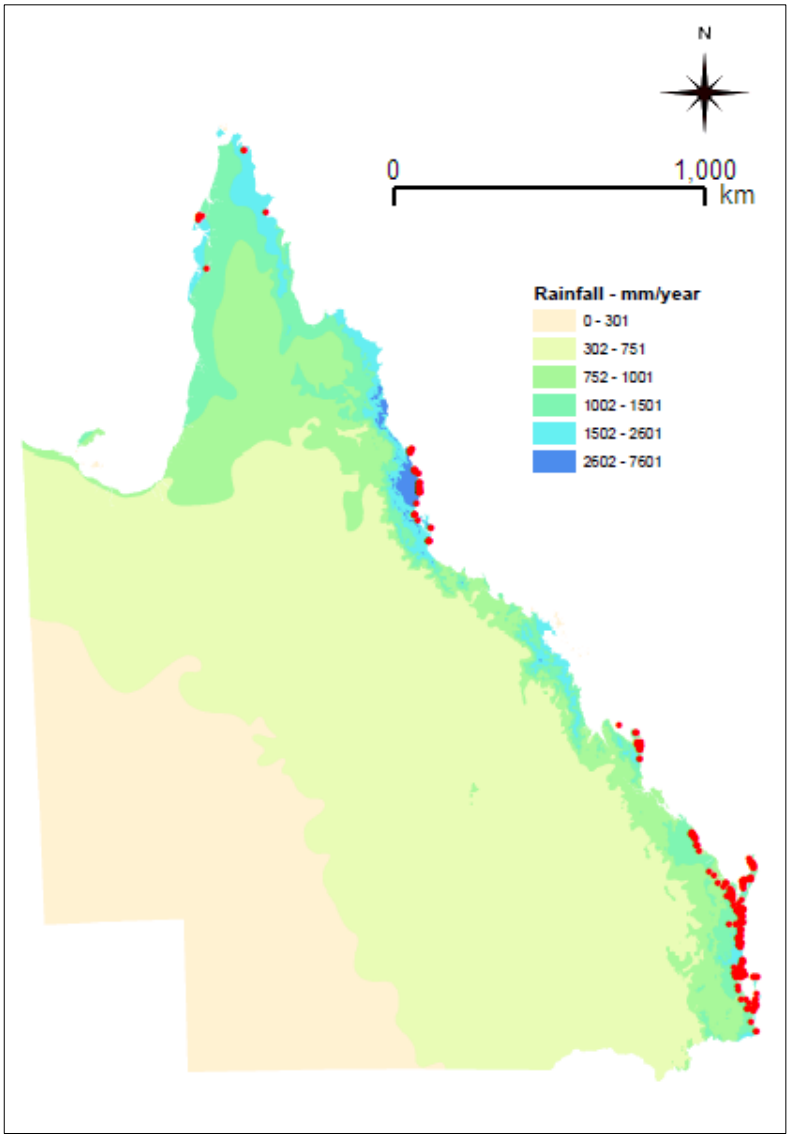

Figure 1. Map of Queensland displaying sites of potential Melaleuca quinquenervia leaf preservation as red circles. Total number of water bodies that fit a set of criteria determining likelihood of leaf preservation in lake sediments number 284. Map produced by R. Mitchell (Department of Science, Information Technology, Innovation and the Arts, Queensland Government), using ESRI ArcMap, via J. Tibby (pers. comm. 2014), later modified.

The known North Stradbroke Island coring site, and other potential sites, are located in areas vulnerable to the variations in climate induced by cycles of ENSO both in the modern and in the past (Donders *et al*. 2007). This study will contribute to gaining a better understanding of what precipitation was like in the geologic past. Variations in

the state of ENSO have occurred in the past, and understanding these can help constrain projections of variations in precipitation in response to future climate change (Latif & Keenlyside 2009).

METHODS

Localities and sample collection

Samples of leaves and stems were collected in March 2014 from 21 locations (20 discrete) around Brisbane, the Sunshine Coast and on North Stradbroke Island (Figure 2). Four sites were later collected from the Cape York Peninsula by a separate group. Two teams initially collected in the Brisbane area, on the Sunshine Coast and on North Stradbroke Island. These two teams were led by Jon Marshall and Glenn McGregor from the Queensland Department of Science, Information Technology, Innovation and the Arts.

Variation in mean annual precipitation across the Southern Queensland region was investigated, with initial estimations of annual rainfall for a number of years previous to 2014 derived from Bureau of Meteorology (BOM) climate records (Bureau of Meteorology 2014). The presence of *Melaleuca quinquenervia* was deduced by analysing geographic information system (GIS) bioregion mapping provided by the Queensland Government. Large areas that showed a dominance of the target species were marked for further analysis, with the goal to sample areas of *Melaleuca quinquenervia* in the most diverse rainfall regimes as possible. Each site was then chosen during field surveying, with small pockets of the target species chosen from the large areas of species dominance.

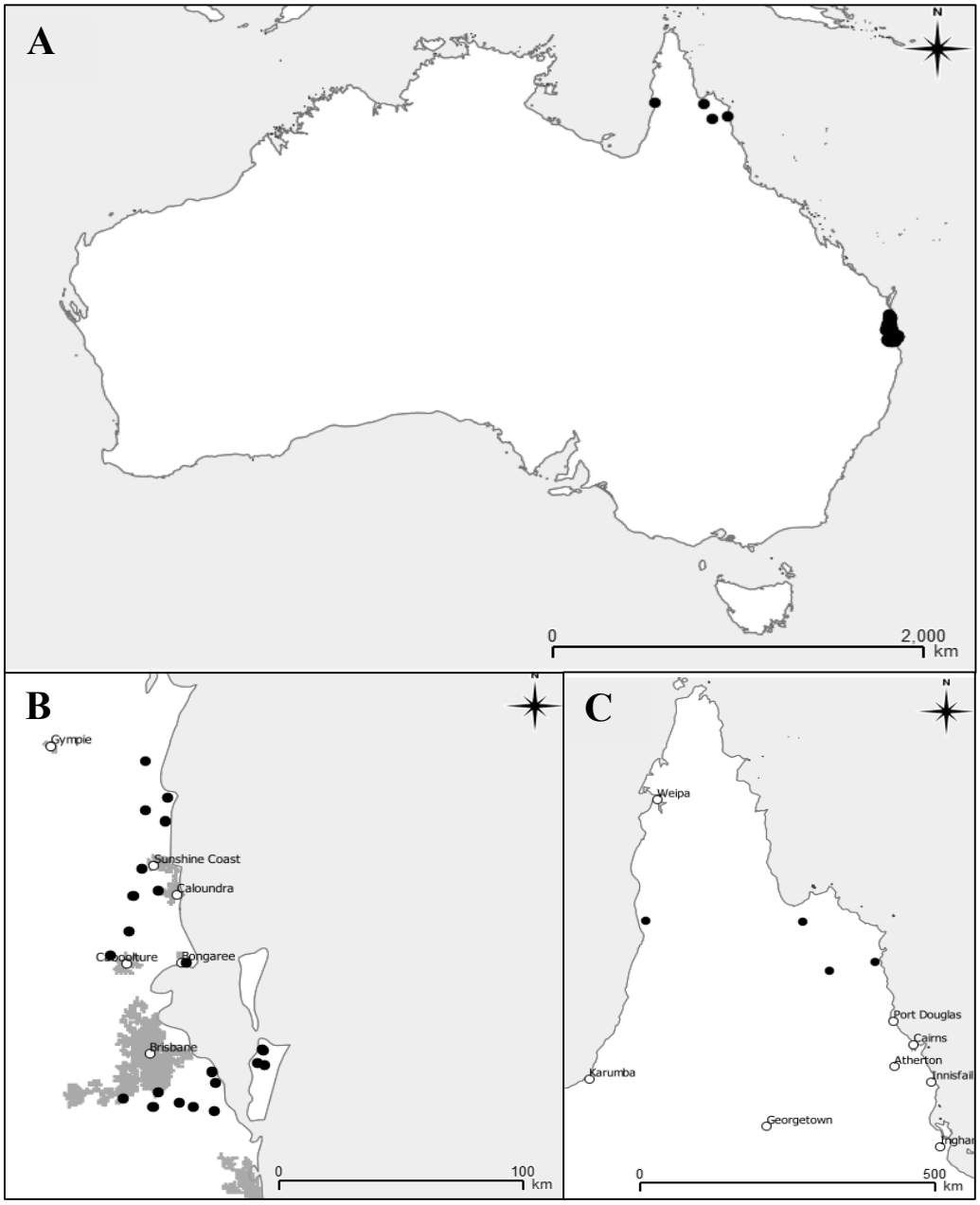

Figure 2. Map of sampling locations. A) In the context of Australia, B) localised Brisbane, North Stradbroke Island and Sunshine Coast regions, and C) Cape York region. Sampling locations are shown in black circles (three replicates per location, two for Cape York), with major population centres and their names shown as white circles. The extent of major urban population can be seen as grey shaded areas. Maps produced using QGIS software and utilising datasets from Natural Earth (2014).

Each particular site was designated a letter and number code based on which team was involved in the collection or, for North Stradbroke Island, which lagoon or water body the sample was collected close to (i.e. G1 (Glenn McGregor, first site collected), J2 (Jon

Marshall, second site collected), BL1 (Brown Lake, first site collected)). Sites where samples were collected were diverse in their nature, and included seasonal wetlands, lakes and lagoons, swamps and creeks. At each of these sites, three trees were chosen as replicates (each replicate was designated a letter: a, b or c, to differentiate between replicates at each site). The location of each tree was GPS located in the WGS 84 reference system. A number of variables were taken into account when deciding on trees to sample. An attempt was made to vary the proximity to water and the tree height of replicates.

For each tree sampled, a large group of leaves were cut from the stem with secateurs. Attempts were made where possible to sample consistent heights (~1-2 metres) and the north facing sides of trees. The sample was put into a paper bag and stapled shut. A number of small leaves (~10-15) were also collected from each tree by picking them off by hand. These were also bagged and stapled.

Leaf preparation

Leaf samples were dried in an oven at 50^{o}C for 48 hours. For all laboratory handling of the samples, any utensils and apparatus used were rinsed three times each with water, reverse osmosis (RO) water and with solvents (methanol, dichloromethane and n-hexane). All glassware had been ashed (subjected to high heat for decontamination) before each new sample was processed.

The nine smallest leaves from each replicate site were qualitatively chosen. Nine were used as this was the number used in an ongoing study of *Melaleuca quinquenervia* that was the basis for this study (C. Barr, pers. comm. 2014). The smallest were chosen in

the hope that these would be the youngest leaves, which had been on the tree for fewer than four years; however this may not be the case. The leaves were measured lengthwise with callipers, and photographed for later reference.

Leaves were then ground to a fine powder using liquid nitrogen in a porcelain mortar and pestle. Leaves were ground with the pestle until the liquid nitrogen poured on top of them had evaporated. If after the first grind there were still large particles of the leaf matter, more liquid nitrogen was added and another grind completed. The fine powdered leaf was then transferred to an ashed 10 millilitre vial.

Bulk $\delta^{13}C$ analysis

The ground samples were weighed for Elemental Analysis – Isotope Ratio Mass Spectrometry (EA-IRMS). Samples of ground leaves from each site were weighed into tin capsules with a goal weight of 0.5 to 1.5 milligrams. The samples in these capsules were then folded into small packages.

Weighed and packaged samples were then analysed for bulk carbon using EA-IRMS by Mark Rollog at the University of Adelaide. The model of EA-IRMS used was a EuroVector EuroEA Elemental Analyser in-line with a Nu Instruments Nu Horizon continuous-flow mass spectrometer. Two unique standards were used in this analysis; glutamic acid and glycine, which were calibrated against international standards. Measured bulk $\delta^{13}C$ was output as values (Appendix 1), with units of per mil (‰). The lab running average precision of the instruments on which these measurements were determined was 0.05‰. These were then converted to discrimination with Formula 2. Values can be found in Appendix 1.

Leaf wax *n*-alkane analysis

Ground plant material was also analysed for the average chain length (ACL) distributions of the leaf wax *n*-alkanes present. Approximately 100 milligrams of ground plant material was weighed into labelled test tubes and subjected to lipid extraction (K. Neilson & F. McInerney pers. comm. 2014, after Collister *et al.* 1994): The samples were sonicated using a Soniclean 250TD ultrasonic bath in approximately 5 to 7 millilitres (mL) of 9:1 volume/volume (v/v) Dichloromethane (DCM): Methanol (MeOH). Each sample was sonicated three times for 15 minutes each time, with a transfer of the solution and a refill of 5 to 7 mL of 9:1 v/v DCM:MeOH to the samples after each sonication. Each transfer was completed using ashed pipettes, with the solution filtered through a folded glass fibre filter in a funnel into a new test tube. Once all transfers had been completed, the resulting total lipid extract (TLE) was then dried down under a stream of dry N_2 gas, and then quantitatively transferred using a DCM rinse (three times).

The TLE was then purified using short column silica gel chromatography. TLE was run through a column (pipette filled with activated silica gel) in solution with 4 mL of hexane. Non-polar lipids including *n*-alkanes were removed in this step, which were then collected in a 4 mL vial. This constituted the first fraction (F1). The remaining compounds in the extract that were held by the column were then flushed through using a 1:1 DCM:MeOH mixture and also collected in a four millilitre vial. This constituted the second fraction (F2).

The F1 was then concentrated under an N_2 gas stream and transferred to inserts inside two millilitre vials, before being concentrated again. Exactly 100 microlitres (μL) of hexane was added to each sample using a calibrated syringe, ready for gas chromatograph - mass spectrometry (GC-MS) analysis.

Samples were analysed by Tony Hall at the University of Adelaide using a Perkin Elmer Clarus 500 Gas Chromatograph-Mass Spectrometer (GC-MS). The column used was an SGE CPSil-5MS (60 m x 0.25 mm ID x 0.25 μdf phase thickness). The carrier gas flow was 1ml/min. The oven temperature program was 50^{o}C, held for one minute, ramped to 340^{o}C at 8^{o}C/minute, and held for 7.75 minutes. 1μL of sample was injected either in split mode (50:1) or splitless mode depending on concentration. The standard used contained only even *n*-alkanes from *n*-C_{14} to *n*-C_{32}, excluding *n*-C_{28}. The mass spectrometer scanned from 45-500 Da, with an injection temperature of 300^{o}C. Four samples were analysed using a HP5973 MS coupled to a HP6890 GC, though the column and run specifications remained unchanged.

After samples were analysed, sample peak areas were integrated, using Turbomass software, for the *n*-C_{25} to *n*-C_{33} range. Values from this process can be found in Appendix 2. This range was chosen due to the abundance maximum for terrestrial plants falling within this range (Brincat *et al*. 2000, Chikaraishi & Naraoka 2003). Average chain length distributions were then calculated as a weighted average using Formula 4 (Bush & McInerney 2013):

$$ACL = \Sigma (C_n \times n) / \Sigma (C_n) \quad (4)$$

With C_n numbers representing the area under the chromatographic peak and *n* numbers the specific chain length. Values from these calculations used to create data plots can be found in Appendix 3.

Climate information

Climate data was derived from SILO, a climate database hosted the Government of Queensland Department of Science, Information Technology, Innovation and the Arts (DSITIA). Datadrill, a tool available through SILO, was used to interpolate the extended sets of data for the specific sample collection sites, with the GPS coordinates of the 'a' replicates used in this data extraction. A number of climate variables available through SILO were extracted from these datasets, and included the maximum and minimum temperature, precipitation, evaporation, vapour pressure and relative humidity at the time of maximum and minimum daily temperatures, all as daily values (Queensland Government 2014).

A statistics software program, R, was then used to analyse and extract relevant data for use in this study. Mean annual precipitation (MAP) and precipitation minus evaporation (P-E) were calculated as an annual average for four years previous of sample collection, and relative humidity (RHmax) and vapour pressure deficit (VPD) were averaged for four years previous of March 2014 inclusive. Winter and spring climate variables were also calculated for the same period of time. The reason for calculations being done for four years previous was due to the maximum life spans of leaves of *Melaleuca quinquenervia* being approximately four years. Mean annual precipitation ranged by 1185.95 mm per year across the sites. All derived climate data can be found in Appendices 4 & 5.

Bulk Δ data calculated from the measured mean bulk $\delta^{13}C$ values of the replicates of each individual site, as well as average chain length of *n*-alkanes, were analysed as a function of a number of climate variables. MAP, P-E, RHmax and VPD were plotted versus Δ, with statistics including regression coefficient (r^2) values and p-values calculated through ANOVA in Microsoft Excel. From these correlations, a calibration was developed that would have the potential to be applied to Δ data obtained from geological records. To calculate this calibration, a regression was applied to a plot of MAP as the response variable (y) and Δ as the predictor variable (x). ACL distributions were calculated using a number of different chain length parameters, with two chosen as the best representative parameters to use for plotting. These were ACL of odd carbon chain lengths from *n*-C25- *n*-C33, and ACL of chain lengths *n*-C27, *n*-C29 and *n*-C31. These were plotted versus climate variables, and the same method as Δ was used to calculate a calibration using ACL distributions.

OBSERVATIONS AND RESULTS

Bulk carbon isotopic composition and carbon isotopic discrimination

Bulk carbon isotopic composition ($\delta^{13}C$) and carbon isotopic discrimination (Δ) are both reported in per mil (‰), and the values for each GPS located site and its replicates (n = 71) can be found in Appendix 1. Bulk $\delta^{13}C$ for each tree ranged from -28.73 ‰ to -34.64‰, with an average composition of -31.56‰. The Δ values of the leaf samples range from 21.35‰ to 27.59‰, with a mean of 24.33‰.

Carbon isotopic discrimination (Δ) for mean of replicates from each site was plotted against a number of climate variables: mean annual precipitation (MAP) and

winter/spring precipitation; and annual and seasonal precipitation minus evaporation (P-E) as well as vapour pressure deficit (VPD) and relative humidity at the time of maximum daily temperature (RHmax). Statistical analyses of the correlations of climatic variables and the mean value of Δ for each site are given in Table 1, with regression coefficient (r^2) and p-values calculated.

For climate variables calculated as an annual average for four years previous of March 2014, two of the four of these correlations show statistical significance (MAP; $r^2 = 0.19$, $p = 0.032$ and P-E; $r^2 = 0.22$, $p = 0.018$) (Table 1).

		Discrimination (Δ)		
		r^2	p	Regression equation
Climate variables annual (calculated for four years from March 2010 to March 2014)	**MAP**	**0.19**	**0.032**	**y = 0.0014x + 21.91**
	P-E	**0.22**	**0.018**	**y = 0.0012x + 24.21**
	RHmax	0.09	0.15	y = 0.1177x + 17.86
	VPD	0.10	0.12	y = -2.3177x + 26.25
		Discrimination (Δ)		
		r^2	p	Regression equation
Climate variables Winter/Spring (calculated for 2010 to 2013)	**W/SP**	0.09	0.13	y = 0.0026x + 23.18
	P-E	0.10	0.12	y = 0.0014x + 24.78
	RHmax	0.10	0.13	y = 0.0962x + 19.38
	VPD	0.09	0.14	y = -1.5548x + 25.61

Table 1. Statistical analyses (r^2 and p-values, and linear regression equations) of average discrimination (Δ) for each site versus climate variables (mean annual precipitation, precipitation-evaporation, relative humidity and vapour pressure deficit). Calculated for annual climate averages across a four year period (March 2010 to March 2014 inclusive), and Winter/Spring climate averages (2010 to 2013). Bold values show correlations with statistical significance ($p < 0.05$).

There is no significant correlation between mean Δ and RHmax or VPD for annual climate variables, and no significant correlations between mean Δ and any variables calculated for winter and spring.

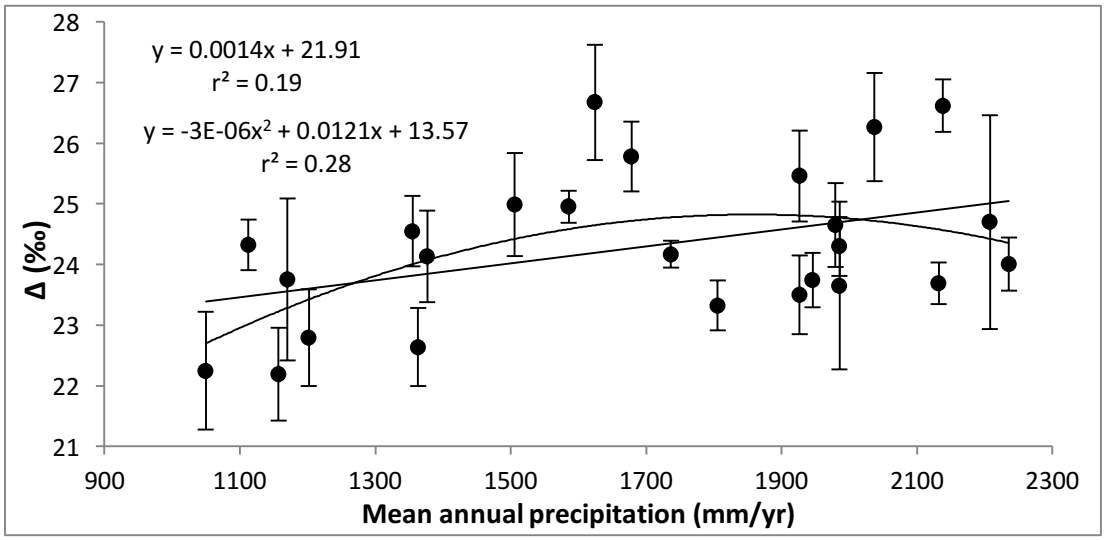

Figure 3. Mean carbon isotopic discrimination (Δ) for each sampling location plotted by mean annual precipitation averaged across a time period of four years from March 2010 to March 2014. Solid black lines indicate a linear regression and a second order polynomial regression for plotted values. Error bars are ± 1 standard deviation.

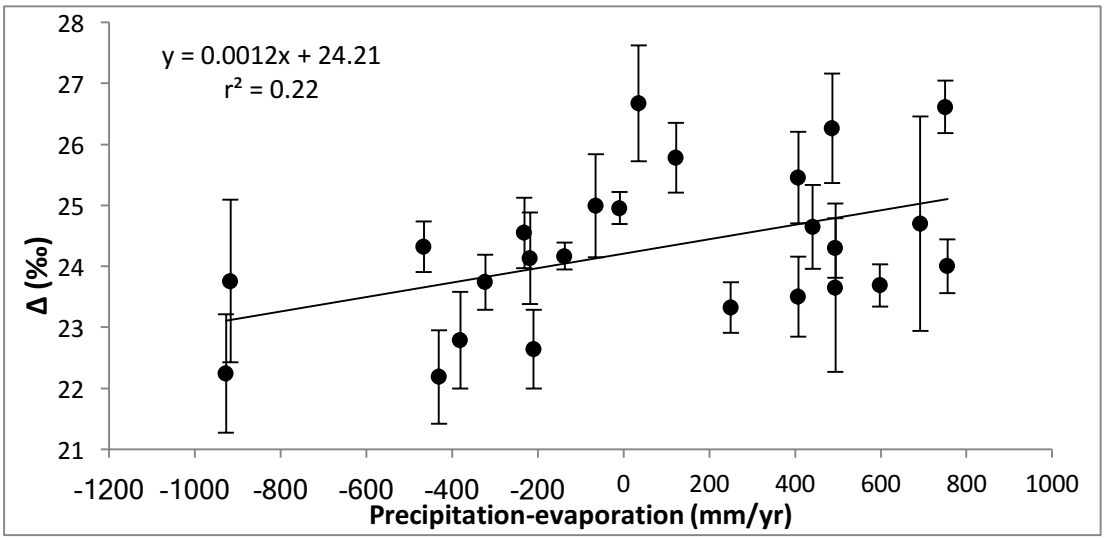

Figure 4. Mean carbon isotopic discrimination (Δ) for each sampling location plotted by mean annual precipitation-evaporation averaged across a time period of four years from March 2010 to March 2014. Solid black line indicates linear regression for plotted values. Error bars are ± 1 standard deviation.

Figures 3 and 4 plot mean Δ for each sampling location against MAP and P-E. Standard deviations from the mean calculated from three replicates for each site range from 0.22‰ to 1.76‰, with a mean of 0.71‰. Each plot shows a positive linear correlation

with an increasing Δ value as climate variables progress from drier to wetter conditions. In the case of P-E, Δ increases across a transition from a negative water balance where there is more evaporation than precipitation, to a positive one, where precipitation dominates over evaporation. P-E shows a better regression correlation against Δ than MAP. Though the data shows a reasonable linear correlation of increasing Δ with increasing MAP, there is a rather distinct polynomial shape to the plot. When a second order polynomial regression is applied, the r^2 value changes significantly, from a linear regression r^2 value of 0.19 to a polynomial r^2 value of 0.28.

Looking at Δ as a function of both MAP and P-E, but more significantly P-E (Figure 5), a particular trend is noticeable where it is possible to fit two separate regressions to the data (Figure 5).

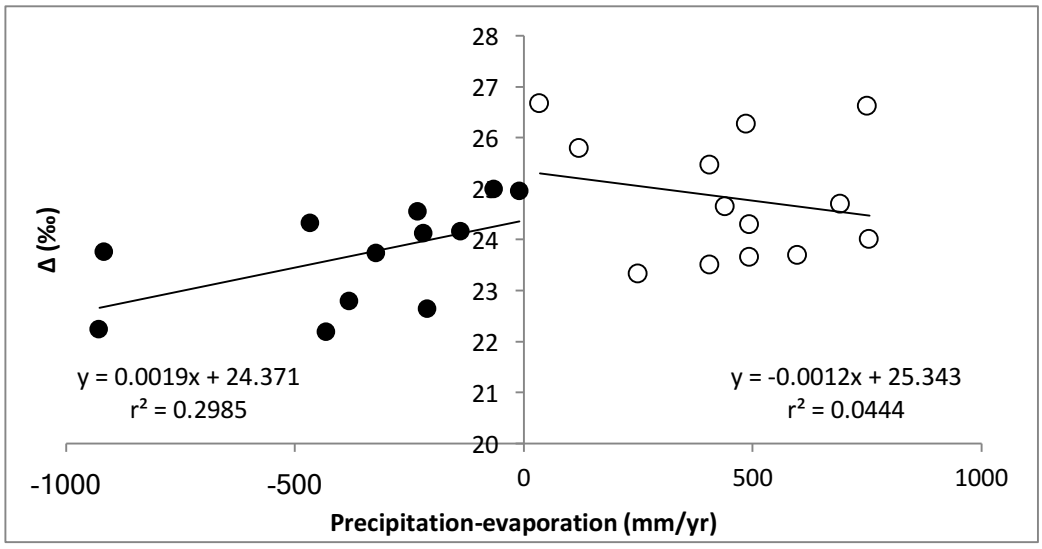

Figure 5. Plot of precipitation-evaporation versus carbon isotope discrimination demonstrating the fitment of two separate linear regressions to the data. Solid black circles display correlations of carbon isotope discrimination values in a negative water balance regime, while open circles display carbon isotope discrimination values in a positive water balance regime.

A linear correlation exists where P-E is less than zero, with a higher regression coefficient value than the full P-E regression ($r^2 = 0.30$), though not significant at the $p<0.05$ level (p-value=0.06). For positive P-E, Δ shows no significant correlation (p= 0.49) and a much lower regression coefficient ($r^2 = 0.044$).

ACL distributions of plant samples

Distributions of chain lengths for leaf samples ranged from *n*-C14 to *n*-C35, though only two samples displayed chain lengths less than *n*-C20 (G3a and G9a), and only four samples displayed chain lengths of *n*-C35 (CY1a, CY2a, CY3a and CY4a). Average chain length was calculated for leaf samples of *Melaleuca quinquenervia,* using Formula 4. For ACL of samples calculated using only the odd chain lengths in the *n*-C25 to *n*-C33 length range, ACL values range between 29.02 and 31.37, with a mean of 30.11. For samples calculated using both odd and even chain lengths in the *n*-C24 to *n*-C33 length range, ACL values range between 28.89 and 31.37 with a mean of 29.98. When ACL is calculated using only the chain lengths *n*-C27, *n*-C29 & *n*-C31, values range between 28.89 and 30.88, with a mean of 30.05. The maximum difference between means calculated using these three different parameters is a length of 0.128. When the parameter of just odd chain lengths is compared to using a parameter of both odd and even chain lengths for the same chain length range, there is only 0.43% difference, a very insignificant amount. Integrated areas under chromatographic peaks and ACL values can be found in Appendix 2 & 3.

Climate variables (calculated for mean annual four years from March 2010 to March 2014)	ACL of odd chain lengths (*n*-C25-*n*-C33)				ACL of odd and even chain lengths (*n*-C24-*n*-C33)				ACL of chain lengths of *n*-C27, *n*-C29 & *n*-C31			
	r^2	p	Regression equation	*n*	r^2	p	Regression equation	*n*	r^2	p	Regression equation	*n*
MAP	**0.19**	**0.034**	**y = -0.0006x + 31.19**	**24**	**0.17**	**0.048**	**y = -0.0007x + 31.11**	**24**	**0.21**	**0.024**	**y = -0.0006x + 31.01**	**24**
P-E	**0.47**	**0.00023**	**y = -0.0008x + 30.15**	**24**	**0.44**	**0.00043**	**y = -0.0009x + 30.02**	**24**	**0.47**	**0.00023**	**y = -0.0007x + 30.09**	**24**
RHmax	0.074	0.20	y = -0.0508x + 32.88	24	0.051	0.29	y = -0.0471x + 32.54	24	0.12	0.096	y = -0.0542x + 33.00	24
VPD	**0.55**	**3.82E-05**	**y = 2.4448x + 28.02**	**24**	**0.53**	**4.98E-05**	**y = 2.6809x + 27.69**	**24**	**0.52**	**7.59E-05**	**y = 1.9782x + 28.36**	**24**
Climate variables (calculated for Winter/spring only for four years from March 2010 to March 2014)	**ACL of odd chain lengths (*n*-C25-*n*-C33)**				**ACL of odd and even chain lengths (*n*-C24-*n*-C33)**				**ACL of chain lengths of *n*-C27, *n*-C29 & *n*-C31**			
	r^2	p	Regression equation	*n*	r^2	p	Regression equation	*n*	r^2	p	Regression equation	*n*
W/SP	**0.62**	**4.36x10-6**	**y = -0.0032x + 31.43**	**24**	**0.58**	**1.60x10-5**	**y = -0.0034x + 31.39**	**24**	**0.59**	**1.19x10-5**	**y = -0.0026x + 31.12**	24
P-E	**0.70**	**3.73x10-7**	**y = -0.0017x + 29.51**	**24**	**0.68**	**7.47x10-7**	**y = -0.0018x + 29.33**	**24**	**0.64**	**3.16x10-6**	**y = -0.0013x + 29.58**	24
RHmax	**0.16**	**0.049**	**y = -0.059x + 33.10**	24	0.14	0.075	y = -0.0597x + 33.01	24	**0.21**	**0.023**	**y = -0.056x + 32.89**	24
VPD	**0.53**	**5.16x10-5**	**y = 1.7008x + 28.65**	24	**0.53**	**5.40x10-5**	**y = 1.8803x + 28.37**	24	**0.50**	**0.00012**	**y = 1.3627x + 28.89**	24

Table 2. Table of statistical values for average chain length distributions correlated with a number of different climatic variables (mean annual precipitation (MAP), precipitation-evaporation (P-E), relative humidity at the maximum daily temperature (RHmax), and vapour pressure deficit (VPD). Climate variables are calculated as mean annual values and winter and spring only averages for four years previous of March 2014. Three parameters are used to calculate average chain length distributions (odd chain lengths for *n*-C25-*n*-C33, odd and even chain lengths for *n*-C24-*n*-C33 and chain lengths of *n*-C27, *n*-C29 & *n*-C31). Bold values stipulate statistically significant linear correlations

Average chain lengths calculated using the parameters outlined show a number of significant correlations, as can be seen in Table 2. The ACL distribution calculations across three ACL parameters are all extremely similar in their regressions, especially when correlated with MAP and P-E annual values. A number of climate variables, calculated for annual climate averages and winter/spring climate averages show significant correlations ($p<0.05$), and these are plotted in Figures 6 and 7 and shown in bold in Table 2. Only ACL calculations using the odd chain length parameter are included as figures in this study. The correlations that are not statistically significant are all ACL calculation parameters versus RHmax when calculated as annual RHmax averages and the odd and even chain length parameter versus RHmax when it is calculated as a winter/spring average; these are not plotted.

Annual averaged MAP shows a statistically significant negative linear relationship with ACL, though shows a stronger correlation ($r^2=0.21$) for ACL values calculated using *n*-C27, *n*-C29 & *n*-C31chain lengths. Winter and spring averaged precipitation (W/SP) versus ACL displays a high statistical significance for all ACL parameter calculations. This relationship shows strong regression coefficients, with the correlation of W/SP when using ACL values calculated with odd chain lengths from *n*-C25-*n*-C33 ($r^2=0.62$). Winter and spring averaged P-E values when correlated with both odd chain length and *n*-C27, *n*-C29 & *n*-C31chain length parameters are highly statistically significant and show well constrained regression coefficients ($r^2=0.70$; $p=3.37\text{x}10^{-7}$ and $r^2=0.64$; $p=3.16\text{x}10^{-6}$, respectively). This is compared to annual P-E average values for both calculation parameters (both $r^2=0.47$; $p=0.00023$), which are still highly statistically significant.

Correlations between ACL values and RHmax are negatively correlated, but are only statistically significant for winter and spring averaged calculations, and even then, show very low regression coefficients compared to other climate variables (r^2=0.16; p=0.049 and r^2=0.21; p=0.023, respectively).

When linear regressions are applied to correlations between VPD and various calculated ACL distributions, all show highly statistically significant positive correlations with reasonably high regression coefficients. This applies to both VPD calculated as an annual average and VPD for winter and spring. Though linear regressions are statistically significant, another regression model may fit the data better. For VPD versus ACL, there is a steep positive trend initially as VPD increases, before plateauing at VPD values greater than approximately one kilo-Pascal (kPa). This trend is better modelled by a natural logarithmic function. For each plot of VPD versus ACL, the regression coefficient increases when this model is used (Figure 6c, and Figure 7d). When odd chain lengths are used as a parameter, annual average VPD versus ACL shows r^2=0.58, and for the same parameter, winter and spring average VPD shows r^2= 0.59.

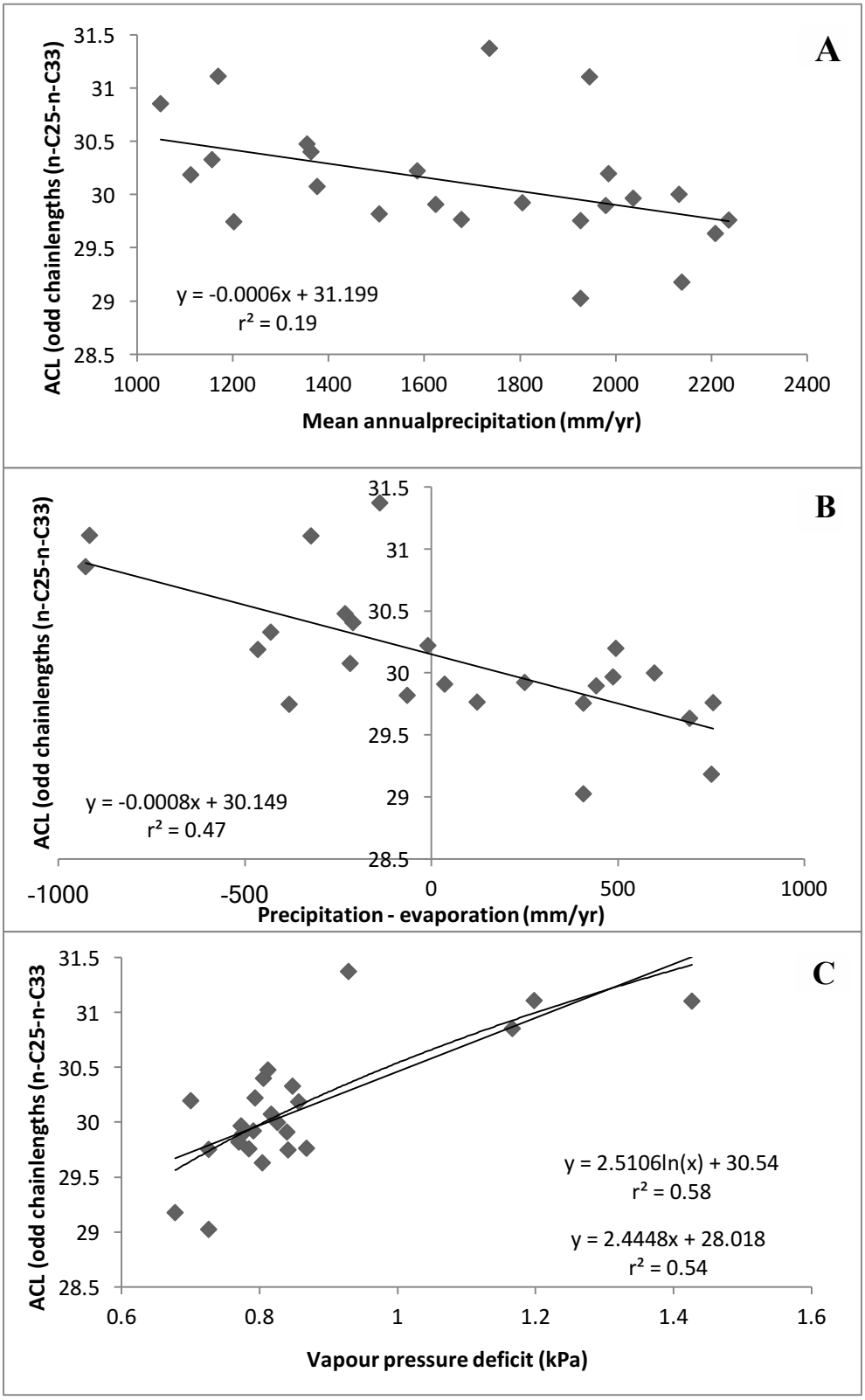

Figure 6. Plots of average chain length of leaf samples versus A) mean annual precipitation, B) precipitation-evaporation and C) vapour pressure deficit. Average chain length distributions are calculated using the parameter of odd chain lengths of *n*-C25 to *n*-C33. Plots show linear regressions, and for ACL vs VPD, both linear and logarithmic regressions are shown.

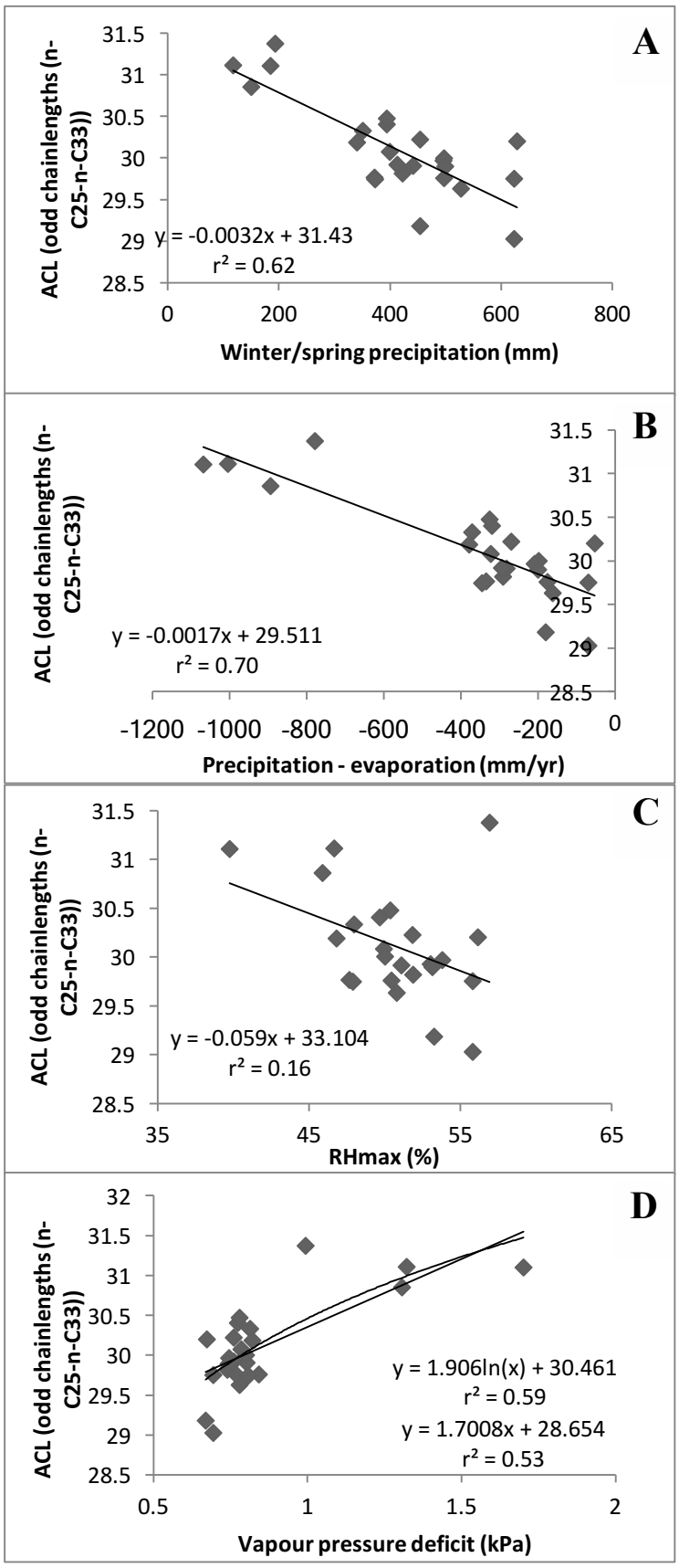

Figure 7. Plots of average chain length of leaf samples versus A) winter and spring precipitation, B) winter and spring precipitation-evaporation and C) relative humidity and D) vapour pressure deficit. Average chain length distributions are calculated using the parameter of odd chain lengths of *n*-C25 to *n*-C33. Plots show linear regressions, and for ACL vs VPD, both linear and logarithmic regressions are shown.

Calibration development

DISCRIMINATION CALIBRATION

A calibration is presented using Δ calculated from $\delta^{13}C$ values measured from leaf samples collected in this study. The calibration is calculated as a linear regression with MAP as a function of Δ, with the regression equation expressed as:

$$\text{Mean annual precipitation} = 132.08(\Delta) - 1518.6 \quad (5)$$

AVERAGE CHAIN LENGTH CALIBRATION

A calibration of MAP as a function of ACL is presented. This calibration has been developed using average chain length values calculated using the parameter of odd chain lengths for the range of *n*-C25-*n*-C33, and is expressed as:

$$\text{Mean annual precipitation} = -291.36(\text{ACL}) + 10450 \quad (6)$$

DISCUSSION

Bulk carbon isotopic composition and carbon isotopic discrimination

Our results show a positive linear correlation between precipitation and Δ (negative linear correlation between precipitation and $\delta^{13}C$), with increasing Δ (smaller $\delta^{13}C$) as water availability increases. This supports the hypothesis that leaves from drier environments have a smaller value of Δ and those from wetter environments a larger Δ. These results are consistent with a number of previous studies looking at how carbon isotopic composition varies with precipitation (Stewart *et al*. 1995; Anderson *et al.* 1996; Miller *et al*. 2001; Weiguo *et al*. 2005; Prentice *et al*. 2010; Ma *et al*. 2012; Wang

et al. 2013). Many of the studies that our results correlate with use $\delta^{13}C$ without calculating to Δ when displaying their results, though $\delta^{13}C$ and Δ will vary approximately opposite to one another for a constant $\delta^{13}C_{atmosphere}$. In an attempt to validate our results and linear model, regression equations of MAP versus $\delta^{13}C$ of five studies from the literature are listed (Table 3) and plotted along with the regression equation derived from the measured $\delta^{13}C$ of our samples versus MAP (Figure 8).

Regression Equation ($\delta^{13}C$ vs MAP)	**Types of samples used for analysis**	**Area of study**	**Study publication/authors**
y = -0.0031x - 24.16	Average plant community leaf samples across a rainfall gradient.	Southern Queensland, Australia	Stewart *et al*. 1995
y = -0.011x -21.70	Leaf samples of C3 plant species *Heteropappus less, Lespedeza sp. and Stipa bungeana*	North-west China	Weiguo *et al*. 2005
y = -0.0178x - 19.38	Foliage samples of various plant species across different vegetation types along a rainfall gradient.	North-east China	Prentice *et al*. 2010
y = -0.006x-25.11	Fully expanded leaves of dominant C3 species at each sampling site.	Northern China	Ma *et al*. 2012
Y = -0.0026x-24.96	Evergreen tree data from the literature	Literature analysis	Wang *et al*. 2013
y = -0.0013x - 29.28	Bulk leaf tissue of *Melaleuca quinquenervia* (average of replicates for each site).	Southern Queensland, Australia	This study (Andrae 2014)

Table 3. Regression equations for a suite of studies from the literature examining the relationship between $\delta^{13}C$ and mean annual precipitation.

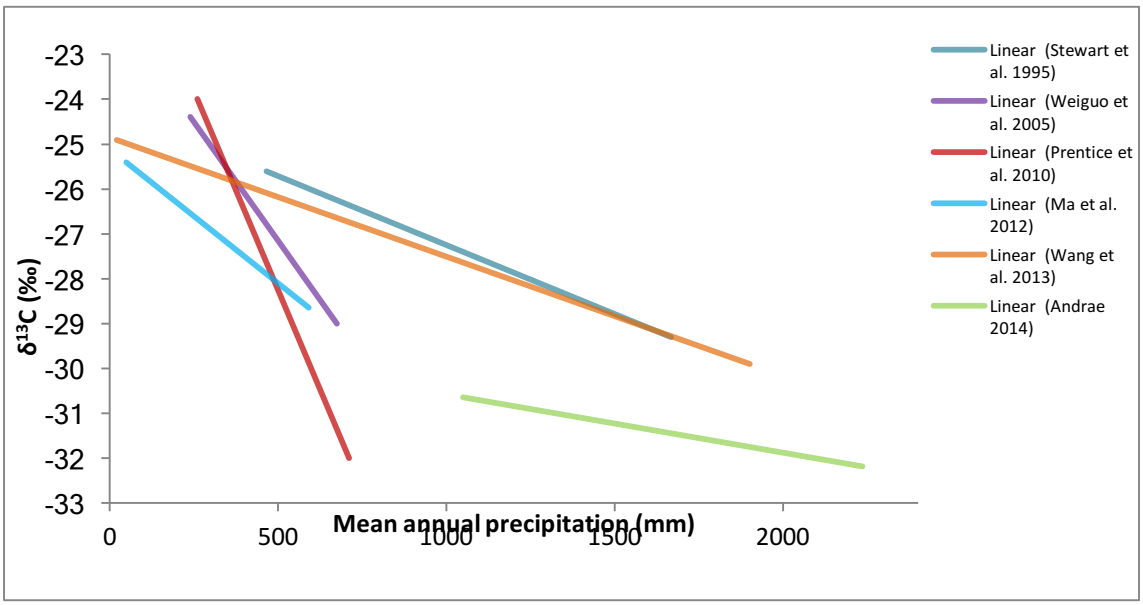

Figure 8. Plot of linear regressions derived from a number of datasets from various studies correlating $\delta^{13}C$ and mean annual precipitation, plotted in carbon isotope composition and precipitation space in relation to one another. Linear regression derived from this study is plotted in green.

A number of studies report that photosynthetic pathway and plant functional type, including if the plant is an angiosperm or gymnosperm, as well as a plant's life habit, significantly influence the carbon isotopic fractionation during carbon uptake by plants (e.g. Troughton 1974; O'Leary 1981, 1988, Leavitt & Newberry 1992; Collister *et al.*1994). A number of the aforementioned studies examine large datasets both from sampling and the literature, with many species of plants, each displaying varying life habits and plant functional types in different growing conditions (e.g. Stewart *et al*. 1995; Prentice *et al*. 2010; Wang *et al*. 2013).

This study examines a single species of tree, *Melaleuca quinquenervia* when looking into correlations between climate variables and the bulk carbon isotopic ratio ($\delta^{13}C$) and subsequently the discrimination (Δ) of bulk leaf tissue of plant samples. Miller *et al*. (2001) studied carbon isotopic discrimination of leaves with declining rainfall for a

number of individual and unique plant species (n=13), and found that five of those thirteen species displayed a decrease in leaf Δ with declining rainfall. Another seven displayed no response, while one showed an increase in Δ as precipitation lessened. This demonstrates the importance of a single species analysis, notably when using that analysis to develop calibrations to be used on sub-fossils of that species. By focussing on the species *Melaleuca quinquenervia*, in a relatively homogenous habitat, it is possible to discern exactly what influence precipitation has on how carbon isotopes are fractionated during carbon uptake by this species. The linear regressions found in previous studies fit the theory of Δ variation with precipitation, as does the same linear analysis applied for a correlation between MAP and $\delta^{13}C$ applied for this study. With this knowledge, confidence in the use of this regression as a calibration is significantly bolstered.

Although a linear regression applied to our data fits well and is consistent with other studies (Stewart *et al*. 1995; Weiguo *et al*. 2005; Prentice *et al*. 2010; Ma *et al*. 2012; Wang *et al*. 2013), it has been reported that models other than linear regressions may better fit correlations between climate (specifically precipitation) and carbon isotopic composition of plant material (Korol *et al*. 1999; Kohn 2010). Korol *et al*. (1999) suggest a negative exponential model for effective rainfall versus Δ, whereby Δ increases sharply with increasing rainfall before reaching a plateau. Kohn (2010) models MAP versus $\delta^{13}C$ using a logarithmic function, where $\delta^{13}C$ is equal to -5.61 $\log_{10}$ (MAP + 300, mm/yr), also suggesting a plateauing of $\delta^{13}C$ values as precipitation increases. Neither of these regressions when applied to our data significantly changes how well the model fits the plot, but when a second order polynomial regression is

applied to the data, the fit is significantly better (Figure 3). Even so, the second order polynomial trend is quite shallow and is not conducive of a model that significantly assists in reinterpreting the data. A large number of studies indicate the use of a linear regression to model correlations between MAP and $\delta^{13}C/\Delta$, rather than any other model.

BULK ISOTOPE CALIBRATION AND TEST OF THIS CALIBRATION

An important aspect of this study is to test the validity of the calibration derived from correlations of MAP and Δ across the sites sampled. In order to achieve this, the calibration that has been developed has been applied to the Δ value (23.3‰) for leaves collected from the top of a core collected from Swallow Lagoon on North Stradbroke Island. This core has been radiocarbon (^{14}C) dated, with the use of 15 reference dating locations throughout the 5.1 metre core (J. Tibby & C. Barr pers. comm. 2014). The leaves from the core-top have been found to date to 1990. The carbon isotopic composition of the atmosphere for this period was -7.8‰ (Cuntz 2011). Climate data has been derived for a period of time four years previous of the date of the deposition of these leaves, from Wallen Wallen meteorological station, with a mean annual rainfall for 1986, 1987, 1988 and 1989 calculated (Bureau of Meteorology 2014). The calculated average of mean annual precipitation for these four years is 1679.3 mm/yr.

When the Δ value for core top leaves is substituted into the calibration (Equation 5), the resulting MAP value derived is 1558.5 mm/yr. This value varies by 7.19 % from the value of measured precipitation for the years of 1986, 1987, 1988 and 1989 measured at Wallen Wallen meteorological station.

PRECIPITATION-EVAPORATION MULTIPLE REGRESSION MODEL

The trend where two separate linear regressions fit the data better than one linear regression (Figure 5) when looking at Δ as a function of P-E has potential implications for understanding the role of source water availability in controlling Δ. This trend may be indicative of samples of *Melaleuca quinquenervia* utilising another source of water, such as groundwater, in addition to precipitation when P-E is greater than zero, and relying more heavily on precipitation when P-E is less than zero. This would explain the greater dependence of Δ on P-E when P-E is less than zero. Grouping of water balance regimes can be seen in Figure 9. This is only a preliminary observation and further research is required.

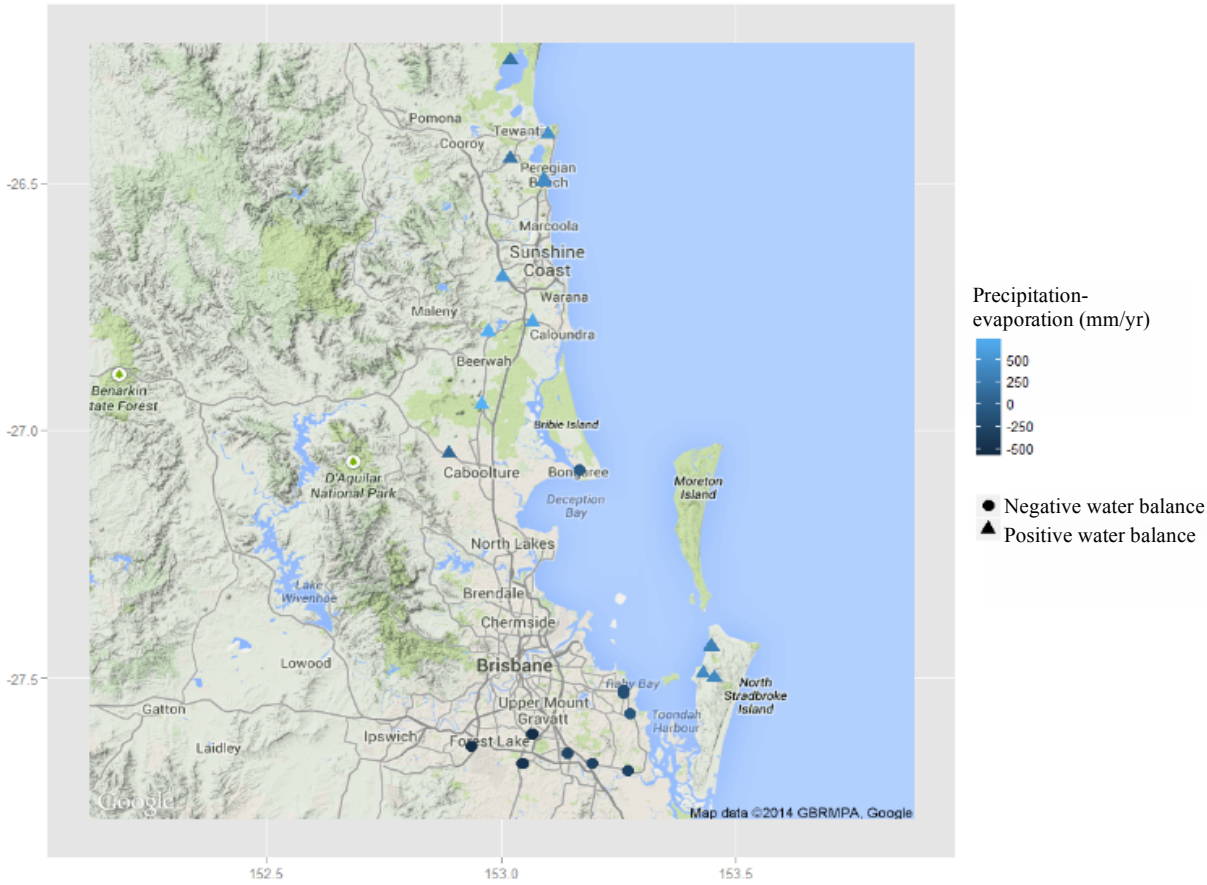

Figure 9. Map displaying precipitation–evaporation water balance regimes of sample sites for Brisbane, the Sunshine Coast and North Stradbroke Island. Sites with negative water balance are displayed as circles, while sites with positive water balance are displayed as triangles. Shade of symbols indicates ranges in values of precipitation-evaporation. Map produced using R and Google Maps as a base map (S. Westra pers. comm. 2014, Google Maps & GBRMPA 2014).

Average chain length

A number of published studies indicate strong correlations of climate and *n*-alkane ACL values for soils and sediments (Dodd & Poveda 2003; Leider *et al*. 2013; Carr *et al*. 2014; F. McInerney pers. comm. 2014). Others indicate correlations of various climate variables with ACL measured from plants (Hoffman *et al*. 2013; Carr *et al.* 2014). As a result, it was hypothesised that ACL would increase in drier environments, and this is displayed by the data presented in this study. This hypothesis was developed on the basis of the theory that in environments of greater aridity, more long-chain *n*-alkanes that are more effective at preventing water loss are produced, thus influencing the chain length distribution and ACL (Dominguez *et al.* 2010; Bush & McInerney 2013).

The results from this study show a strong correlation between measured leaf ACL and aridity and agree with a number of other studies. Mean annual precipitation and winter and spring precipitation showed a statistically significant negative linear correlation with ACL, with seasonal precipitation even more strongly correlated. Hoffman *et al*. (2013) found a statistically significant negative correlation between annual precipitation and ACL in Acacia species, though found an inverse trend in Eucalypt species. Hoffman et al. found statistically significant trends relationships between relative humidity and ACL, for both Acacia and Eucalypt species. The results from this study show no significant relationship between ACL and relative humidity.

Carr *et al*. (2014) finds a weak but statistically significant correlation of aridity index and ACL, (r^2 0.14, $p < 0.01$), This study correlates leaf ACL with annual and winter and spring precipitation-evaporation, a similar premise to aridity index, as it indicates

the dryness associated with the balance of precipitation and evaporation. Statistically significant and strong correlations exist for both annual and seasonal precipitation-evaporation with ACL.

Strong positive linear correlations of VPD and ACL for both annual and seasonal climate data are presented in this study. A study by Tipple & Pagani (2013) found that although VPD by itself did not significantly contribute to variation in ACL distribution, it was significantly loaded on the first component of a principle component analysis along with mean annual temperature, δD (deuterium isotope ratio) of mean annual precipitation and relative humidity. The results from this study suggest VPD may significantly contribute to ACL distributions.

Correlations between climate and ACL show better relationships and are much more statistically significant than correlations of climate and Δ, indicated by their regressions and p-values. As with other studies including Hoffman *et al.* (2013) and Carr *et al*. (2014), this has implications for the applications as a climate proxy. Calibrations calculated from the correlations between ACL and climate variables, with a strong emphasis on precipitation, have the potential to be used to reconstruct precipitation in the geologic past.

The application of this calibration to reconstruct climate is dependent on how ACL is preserved in the geologic record. This calibration has been developed using one species of plant, *Melaleuca quinquenervia*, and as such, care might be taken to utilise this calibration on ACL records that are proven to be primarily derived from this species.

For reconstructing climate from lake sediment records, measurements of ACL from whole or fragmented leaves may be difficult to obtain. Reconstruction may rely on *n*-alkanes preserved in sedimentary records, and if this is the case, knowledge of the source of the leaf waxes preserved is necessary for the application of the calibration to be considered reasonable. Various paleo-environmental as well as source determination studies analyse leaf wax *n*-alkanes preserved in sediments (e.g. Meyers & Ishiwatari 1993; Brincat *et al.* 2000; Chikaraishi & Naraoka 2003; Chikaraishi *et al*. 2004). These studies attribute leaf wax *n*-alkane distributions for various plant classes (e.g. woody plants versus graminoids) as well as variations in distributions between terrestrial and aquatic plants. This is useful in determining sources of *n*-alkanes for sedimentary ACL records, and may help in the confidence that sedimentary ACL records are derived primarily from *Melaleuca quinquenervia*. If so, the calibration developed using modern measured values of ACL from *Melaleuca quinquenervia* can be applied as a proxy to preserved lipids in the sediment core of Swallow Lagoon and other potential biomarker preservation sites.

CONCLUSIONS

Measured bulk carbon isotope composition ($\delta^{13}C$) and calculated carbon isotope discrimination (Δ) are presented in the context of a spatial precipitation gradient spanning areas around Brisbane, North Stradbroke Island and Cape York Peninsula. A number of significant correlations exist between Δ and climate variables, with statistically significant linear correlations ($p=<0.05$) of Δ with precipitation and precipitation-evaporation. For MAP, a polynomial regression displays a better regression coefficient. Precipitation-evaporation displays an interesting trend where two

regression fit the data, with negative precipitation-evaporation showing a stronger correlation (r^2=0.29), though not statistically significant at the $p<0.05$ level.
Also presented are ACL data calculated for a number of chain length parameters in the context of the same precipitation gradient. Strong and statistically significant negative linear correlations of ACL with mean annual precipitation and winter and spring rainfall, as well as precipitation-evaporation exist. Strongly correlated and statistically significant VPD and ACL also exist, though no significant relationship exists between ACL and RHmax.

Calibrations using both methods of proxy development as a basis have the potential to be applied to leaf material and leaf wax n-alkanes preserved in lake sediments in a number of location throughout Queensland. The power of these calibrations is increased because of the ability for both to be applied to the same core, thus increasing the confidence of any climate reconstructions obtained. This measurement of these modern climate proxies and subsequent development of calibrations has exciting implications for interpreting records of precipitation and determining patterns of ENSO in Australia for the geologic past.

ACKNOWLEDGMENTS

I would like express my gratitude to Francesca McInerney, my supervisor for this Honours thesis, and say thankyou for her great support and sharing of her expert knowledge of isotopes, plant ecology and palaeoclimate. I would like to express my appreciation for the organisation of this Honours year by Ros King and Katie Howard. John Tibby and Cameron Barr were great sources of expertise on the topic of ENSO and precipitation reconstructions, and provided excellent support throughout the year, as well as assisting with collection of samples. Jonathan Marshall, Glenn McGregor and Tim Page were also extremely helpful in assisting with sample collection and sharing their expertise on the ecology of southern Queensland and the dune islands. Both Mark Rollog and Tony Hall were of great assistance in the isotope and chemical analysis of samples, and helped to increase my knowledge of isotope geochemistry extensively. I would like to thank Seth Westra for his significant contribution to the climate and statistical analyses. I would also like to thank Kristine Neilson for her assistance in the lab, and other members of Dr. Francesca McInerney's lab group, who provided insightful comments on the project and moral support.

REFERENCES

ANDERSON, J.E., WILLIAMS, J., KRIEDEMANN, P.E., AUSTIN, M.P. & FARQUHAR, G.D. 1996. Correlations between carbon isotope discrimination and climate of native habitats for diverse Eucalypt taxa growing in a common garden. *Australian Journal of Plant Physiology* **23**, 311-320.

BRINCAT, D., YAMADA, K., ISHIWATARI, R., UEMURA, H. & NARAOKA, H. 2000. Molecular-isotopic stratigraphy of long-chain *n*-alkanes in Lake Baikal Holocene and glacial age sediments. *Organic Geochemistry* **31**, 287-294.

BUREAU OF METEOROLOGY 2014. Climate data online. <http://www.bom.gov.au/climate/data/index.shtml> (retrieved 20 March 2014).

BUSH, R.T. & MCINERNEY, F.A. 2013. Leaf wax n-alkane distributions in and across modern plants: Implications for paleoecology and chemotaxonomy. *Geochimica et Cosmochimica Acta* **117**, 161-179.

CARR, A.S., BOOM, A., GRIMES, H.L., CHASE, B.M., MEADOWS, M.E. & HARRIS, A. 2014. Leaf wax n-alkane distributions in arid zone South African flora: Environmental controls, chemotaxonomy and palaeoecological implications. *Organic Geochemistry* **67**, 72-84.

CASTAÑEDA, I.S. & SCHOUTEN, S. 2011. A review of molecular organic proxies for examining modern and ancient lacustrine environments. *Quaternary Science Reviews* **30**, 2851-2891.

CERNUSAK, L.A., UBIERNA, N., WINTER, K., HOLTUM, J.A.M., MARSHALL, J.D. & FARQUHAR, G.D. 2013. Environmental and physiological determinants of carbon isotope discrimination in terrestrial plants. *New Phytologist* **200**, 950-965.

CHIKARAISHI, Y. & NARAOKA, H. 2003. Compound-specific δD–δ13C analyses of *n*-alkanes extracted from terrestrial and aquatic plants. *Phytochemistry* **63**, 361-371.

CHIKARAISHI, Y., NARAOKA, H. & POULSON, S.R. 2004. Hydrogen and carbon isotopic fractionations of lipid biosynthesis among terrestrial (C3, C4 and CAM) and aquatic plants. *Phytochemistry* **65**, 1369-1381.

COLLISTER, J.W., RIELEY, G., STERN, B., EGLINTON, G. & FRY, B. 1994. Compound-specific $\delta^{13}C$ analyses of leaf lipids from plants with differing carbon dioxide metabolisms. *Organic Geochemistry* **21**, 619-627.

CORNIC, G. 2000. Drought stress inhibits photosynthesis by decreasing stomatal aperture – not by affecting ATP synthesis. *Trends in Plant Science* **5**, 187-188.

CUNTZ, M. 2011. A dent in carbon's gold standard. *Nature Letters* **477**, 547-548.

DIEFENDORF, A.F., MUELLER, K.E., WING, S.L., KOCH, P.L. & FREEMAN, K.H. 2010. Global patterns in leaf ^{13}C discrimination and implications for studies of past and future climate. *Proceedings of the National Academy of Sciences* **107**, 5738-5743.

DODD, R.S. & POVEDA, M.M. 2003. Environmental gradients and population divergence contribute to variation in cuticular wax composition in Juniperus communis. *Biochemical Systematics and Ecology* **31**, 1257-1270.

DOMINGUEZ, E., HERDIA-GUERRERO, J.A. & HEREDIA, A. 2010 .The biophysical design of plant cuticles: an overview. *New Phytologist* **189**, 1-12.

DONDERS, T.H., HABERLE, S.G., HOPE, G., WAGNER, F. & VISSCHER, H. 2007. Pollen evidence for the transition of the Eastern Australian climate system from the post-glacial to the present-day ENSO mode. *Quaternary Science Reviews* **26**, 1621-1637.

EGLINTON, T.I. & EGLINTON, G. 2008. Molecular proxies for palaeoclimatology. *Earth and Planetary Science Letters* **275**, 1-16.

FARQUHAR, G.D., O'LEARY, M.H. & BERRY, J.A. 1982. On the relationship between carbon isotope discrimination and the intercellular carbon dioxide concentration in leaves. *Australian Journal of Plant Physiology* **9**, 121-137.

FARQUHAR, G.D., EHLERINGER, J.R. & HUBICK, K.T. 1989a. Carbon isotope discrimination and photosynthesis. *Annual Review of Plant Physiology and Plant Molecular Biology* **40**, 503-537.

FARQUHAR, G.D., HUBICK, K.T., CONDON, A.G. & RICHARDS, R.A. 1989b. Carbon isotope fractionation and plant water-use efficiency. *In*: Rundel, P.W., Ehleringer, J.R. & Nagy, K.A. eds., *Stable Isotopes in Ecological Research (*1st edition) pp 21-40*, in series: Ecological studies* **68**.

GOOGLE MAPS & GBRMPA (GREAT BARRIER REEF MARINE PARK AUTHORITY) 2014. Brisbane/Sunshine Coast region topographical map. <https://www.google.com.au/maps/@-27.1286362,152.5763139,9Z> (retrieved 28 August 2014)

HOFFMAN, B., KAHMEN, A., CERNUSAK, L.A., ARNDT, S.K. & SACHSE, D. 2013. Abundance and distribution of leaf wax *n*-alkanes in leaves of Acacia and Eucalyptus trees along a strong humidity gradient in northern Australia. *Organic Geochemistry* **62**, 62-67.

JETTER, R., KUNST, L. & SAMUELS, A.L. 2006. Composition of plant cuticular waxes. *In*: Riederer, M. & Müller, C. eds., *Biology of the Plant Cuticle* (1st edition), pp 182-215, Blackwell Publishing, Oxford.

KOHN, M.J. 2010. Carbon isotope compositions of terrestrial C3 plants as indicators of (paleo)ecology and (paleo)climate. *Proceedings of the National Academy of Sciences* **107**, 19691-19695.

KOROL, R.L., KIRSCHBAUM, M.U.F., FARQUHAR, G.D. & JEFFREYS, M. 1999. Effects of water status and soil fertility on the C-isotope signature in *Pinus Radiata*. *Tree Physiology* **19**, 551-562.

LATIF, M. & KEENLYSIDE, N.S. 2009. El Niño/Southern Oscillation response to global warming. *Proceedings of the National Academy of Sciences* **106**, 20578-20583.

LEAVITT, S.W. & NEWBERRY, T. 1992. Systematics of stable-carbon isotopic differences between gymnosperm and angiosperm trees. *Plant Physiology (Life Science Advances)* **11**, 257-262.

LEIDER, A., HINRICHS, K., SCHEFUß, E. & VERSTEEGH, G.J.M. 2013. Distribution and stable isotopes of plant wax derived n-alkanes in lacustrine, fluvial and marine surface sediments along an Eastern Italian transect and their potential to reconstruct hydrological cycle. *Geochimica et Cosmochimica Acta* **117**, 16-32.

MA, J., SUN, W., LIU, X. & CHEN F. 2012. Variation in the stable carbon and nitrogen isotope composition of plants and soil along a precipitation gradient in Northern China. *PLOS One* **7**, 1-7.

MARSHALL, J.D., BROOKS, J.R. & LAJTHA, K. 2007. Sources of variation in the stable isotopic composition of plants. *In:* Michener R. & Lajtha K. eds., *Stable Isotopes in Ecology and Environmental Science* (2nd edition), pp 22-60, Blackwell Publishing, Carlton.

MEYERS, P.A. & ISHIWATARI, R. 1993. Lacustrine organic geochemistry – an overview of indicators of organic matter sources and diagenesis in lake sediments. *Organic Geochemistry* **7**, 867-900.

MILLER, J.M., WILLIAMS, R.J. & FARQUHAR, G.D. 2001. Carbon isotope discrimination by a sequence of Eucalyptus species along a subcontinental rainfall gradient in Australia. *Functional Ecology* **15**, 222-232.

NATURAL EARTH 2014. Large scale cultural, physical and raster data (1:10m). <http://www.naturalearthdata.com/downloads/> (retrieved 24 June 2014).

O'LEARY, M.H. 1981. Carbon isotope fractionation in plants, *Phytochemistry* **20**, 553-567.

O'LEARY, M.H. 1988. Carbon isotopes in photosynthesis. *BioScience* **38**, 328-355.

PRENTICE, I.C., MENG, T., WANG, H., HARRISON, S.P., NI, J. & WANG, G. 2010. Evidence of a universal scaling relationship for leaf CO_2 drawdown along an aridity gradient, *New Phytologist* **190**, 169-180.

QUEENSLAND GOVERNMENT 2014. DSITIA SILO climate data. <https://www.longpaddock.qld.gov.au/silo> (retrieved 2 April 2014)

ROBINSON, M. & DOWSETT, H. 2010. *Why study palaeoclimate?* U.S. Geological Survey Fact Sheet 2010–3021, < http://pubs.usgs.gov/fs/2010/3021/> (retrieved 3 May 2014).

STEWART, G. R., TURNBULL, M. H., SCHMIDT, S. & ERSKINE, P. D. 1995. ^{13}C natural abundance in plant communities along a rainfall gradient: a biological integrator of water availability, *Functional Plant Biology* **22**, 51-55.

TIPPLE, B.J. & PAGANI, M. 2013. Environmental control on eastern broadleaf forest species' leaf wax distributions and D/H ratios. *Geochimica et Cosmochimica Acta* **111**, 64-77.

TROUGHTON, J.H., CARD, K.A. & HENDY, C.H. 1974. Photosynthetic pathways and carbon isotope discrimination by plants. *Carnegie Institution Annual Report of the Director Department of Plant Biology*, *1973-74*. *In:* Carnegie Institution Yearbook **73**, 768-779.

VAN DE WATER, P.K., LEAVITT, S.W. & BETANCOURT, J.L. 2002. Leaf $\delta^{13}C$ variability with elevation, slope aspect, and precipitation in the southwest United States. *Oecologia* **132**, 332-343.

WANG, N., XU, S.S., JIA, X., GAO, J., ZHANG, W.P., QIU, Y.P. & WANG, G.X. 2013. Variations in foliar stable carbon isotopes among functional groups and along environmental gradients in China – a meta-analysis. *Plant Biology* **15**, 144-151.

WEIGUO, L., XIAHONG, F., YOUFENG, N., QUINGLE, Z., YUNNING, C. & ZHISHENG, A. 2005. $\delta^{13}C$ variation of C3 and C4 plants across an Asian monsoon rainfall gradient in arid northwestern China. *Global Change Biology* **11**, 1094-1100.

APPENDIX

List of figures

Appendix 1. Table of site and replicate names, site coordinates, measured bulk carbon isotopic composition ($\delta^{13}C$) and calculated carbon isotopic discrimination (Δ).

Site Name	Replicate Number	Longitude E	Latitude S	Bulk $\delta^{13}C$ (‰)	Mean replicates Bulk $\delta^{13}C$ (‰)	Δ (‰)	Mean of replicates Δ (‰)	σ
BL1	a	153.431	27.490	-31.27	-31.53	24.02	24.30	0.48
(Brown Lake)	b	153.431	27.490	-31.27		24.02		
	c	153.431	27.490	-32.06		24.86		
G10	a	153.167	27.080	-32.85	-33.77	25.69	26.67	0.95
	b	153.167	27.080	-33.84		26.74		
	c	153.167	27.080	-34.64		27.59		
G1	a	153.141	27.651	-29.70	-29.96	22.37	22.64	0.65
	b	153.141	27.651	-29.52		22.17		
	c	153.141	27.651	-30.66		23.38		
G2	a	153.195	27.671	-32.19	-31.37	24.99	24.13	0.75
	b	153.195	27.671	-31.07		23.81		
	c	153.195	27.671	-30.86		23.59		
G3	a	153.271	27.686	-31.18	-31.77	23.93	24.55	0.58
	b	153.271	27.686	-32.26		25.07		
	c	153.271	27.686	-31.86		24.65		
G4	a	153.275	27.570	-31.89	-32.15	24.67	24.95	0.26
	b	153.275	27.570	-32.37		25.19		
	c	153.275	27.570	-32.20		25.00		
G5	a	153.262	27.530	-33.10	-32.18	25.96	24.99	0.85
	b	153.261	27.525	-31.66		24.44		
	c	153.262	27.525	-31.79		24.57		
G6	a	153.067	26.781	-30.01	-31.91	22.69	24.70	1.76
	b	153.067	26.781	-32.63		25.46		
	c	153.067	26.781	-33.10		25.95		
G7	a	152.973	26.801	-31.10	-31.26	23.85	24.01	0.44
	b	152.973	26.801	-30.94		23.67		
	c	152.972	26.801	-31.73		24.50		
G8	a	152.959	26.947	-33.34	-33.72	26.21	26.62	0.43
	b	152.959	26.947	-34.15		27.07		
	c	152.959	26.947	-33.66		26.56		

G9	a	152.889	27.046	-32.31	-32.93	25.12	25.78	0.57
	b	152.889	27.047	-33.25		26.11		
	c	152.889	27.047	-33.25		26.12		
J1	a	153.066	27.611	-29.70	-29.53	22.37	22.19	0.76
	b	153.067	27.611	-28.73		21.35		
	c	152.937	27.636	-30.16		22.85		
J2	a	152.937	27.636	-31.98	-31.55	24.77	24.32	0.42
	b	152.936	27.636	-31.47		24.23		
	c	153.067	27.611	-31.21		23.95		
J3	a	153.045	27.672	-29.40	-30.11	22.04	22.79	0.79
	b	153.047	27.671	-30.89		23.62		
	c	153.046	27.671	-30.03		22.71		
J4	a	153.003	26.691	-31.33	-30.95	24.08	23.69	0.35
	b	153.003	26.691	-30.72		23.44		
	c	153.003	26.690	-30.82		23.55		
J5	a	153.019	26.250	-30.22	-30.61	22.92	23.32	0.41
	b	153.019	26.450	-30.60		23.31		
	c	153.020	26.451	-31.01		23.74		
J6	a	153.100	26.401	-32.50	-33.39	25.33	26.27	0.90
	b	153.100	26.401	-33.48		26.36		
	c	153.100	26.401	-34.18		27.11		
J7	a	153.091	26.493	-31.63	-31.86	24.40	24.65	0.69
	b	153.091	26.498	-32.60		25.43		
	c	153.091	26.498	-31.36		24.12		
SL1	a	153.454	27.498	-31.27	-30.92	24.02	23.65	1.38
(Swallow Lagoon)	b	153.454	27.499	-32.02		24.81		
	c	153.454	27.499	-29.47		22.13		
WL1	a	153.450	27.437	-30.51	-30.78	23.22	23.50	0.65
(Wellsby Lagoon 1)	b	153.450	27.437	-30.34		23.04		
	c	153.450	27.437	-31.48		24.25		
WL2	a	153.447	27.435	-31.85	-32.63	24.63	25.46	0.75
(Wellsby Lagoon 2)	b	153.447	27.435	-32.80		25.64		
	c	153.447	27.435	-33.24		26.11		
CY1	a	144.078	14.764	-30.12	-31.02	22.81	23.76	1.33
	b	144.079	14.764	-31.91		24.70		
CY2	a	145.194	15.463	-31.56	-31.41	24.32	24.17	0.22
	b	145.193	15.462	-31.26		24.01		
CY3	a	144.483	15.612	-28.93	-29.59	21.56	22.24	0.97
	b	144.483	15.612	-30.24		22.93		
CY4	a	141.692	14.758	-31.30	-31.00	24.06	23.74	0.45
	b	141.692	14.758	-30.70		23.42		

Appendix 2. Integrated areas under chromatographic peaks for various chain lengths.

Replicates	Area under the peak for particular chain length															
	C20	**C21**	**C22**	**C23**	**C24**	**C25**	**C26**	**C27**	**C28**	**C29**	**C30**	**C31**	**C32**	**C33**	**C34**	**C35**
G1a					1987.069	8754.081	7485.563	43968.45	8764.717	124153.3	11563.49	478112.5	5513.82	32607.12		
G2a	9825.525	16794.58	24857.82	33316.07	33682.67	57371.63	47699.9	164871.8	78494.95	428557.8	53712.23	1028779	28937.28	105385.4	3765.342	
G3a	254.22	66.622	234.176	316.585	309.333	322.112	272.62	4036.235	1282.302	22532.29	886.164	73979.72	290.168	4008.328		
G4a				49763.09	74322.36	133900.3	155372.1	479828.2	273795.9	1929782	191470.2	4573500	80567.95	373283.6	7417.31	
G5a				1243.586	1694.849	4600.966	4376.922	22727.85	8225.294	45832.5	1369.927	85917.15	205.959	6869.996		
G6a	635.279	175.988	476.203	1216.147	2084.386	4956.514	5683.978	26206.38	7806.553	42995.13	1304.802	74385.31	231.636	5122.704		
G7a	114.713	48.104	130.746	176.094	312.433	416.425	303.108	6275.984	930.617	14178.42	114.767	23762.11	11.142	158.8		
G8a	575.7	102.935	365.413	171.151	474.382	705.488	836.44	7138.61	1777.573	13059.07	55.699	11016.21	22.252	204.215		
G9a	2384.788	678.209	2489.581	2529.718	2974.57	3074.574	2714.241	15962.83	5373.375	49724.27	1910.475	70809.27	229.399	2783.751		
G10a	1390.646	468.969	1463.32	1860.955	2557.16	5374.804	5913.366	33535.65	7644.501	59065.68	2209.077	128570.4	835.11	12008.16		
J1a	56.734	286.537	11.223	458.857	967.614	2791.172	2207.328	13745.65	1726.334	23591.15	847.743	105311	455.902	7984.652		
J2a			234.75	525.772	830.06	2041.854	1459.063	8367.321	2255.702	22978.62	583.777	62058.5	197.222	5013.466		
J3a	834.673	157.507	465.762	970.538	1139.697	4637.233	3805.491	21259.07	3692.872	25150.03	453.205	69250.08	39.747	3756.461		
J4a	513.393	485.492	1005.689	1765.372	1873.048	4590.432	3624.942	18192.38	4808.608	32505.6	664.243	87103.95	304.967	7609.254		
J5a	381.083	384.347	424.443	1199.635	1751.009	5255.699	8116.085	32519.27	6515.398	40902.54	2014.095	123134.8	419.711	8275.784		
J6a	275.444	124.885	203.416	190.228	255.856	350.337	184.439	2318.821	319.214	10565.13	44.439	16502.07	44.929	579.259		
J7a				48.397	68.199	536.631	324.513	11485.4	1196.777	25572.22	22.619	49155.6	11.363	1432.111		
SL1a	11.324	11.324	11.376	11.326	11.376	163.419	119.919	7004.975	357.595	29519.32	58.721	68621.87	0	1235.036		
WL1a	11.273	11.273	11.327	30.837	189.221	1407.317	1507.324	13940.99	914.985	12986.6	22.6	11839.03	124.35	2714.696		
WL2a	22.686	11.369	11.371	34.057	136.376	1074.548	594.706	9993.126	278.794	15251.13	11.371	33812.86	0	575.419		
CY1a	1750	1278	1997	1188	468	6713	1282	41067	1153	191526	10387	2472101	32872	468054	584	11594
CY2a	1194	971	916	2020	1289	12898	614	47295	1257	207888	29961	4850266	95205	1581022	1643	33823
CY3a	1973	1286	925	1075	1162	46748	6495	83419	2732	224710	27433	2209441	52123	321334	2044	10119
CY4a	6395	952	693	2804	1585	11674	6352	24587	5350	108033	15714	2316766	36700	338044	1634	14248

Appendix 3. Calculation of ACL for sites using various parameters

Site Name/replicate	ACL of odd chain lengths (n-C25-n-C33)	ACL of odd and even chain lengths (n-C24-n-C33)	ACL of chain lengths n-C25, n-C27 & n-C29	ACL of chain lengths n-C27, n-C29 & n-C31	ACL of chain lengths n-C29 & n-C31	Average chain length ratio for n-C31/n-C29
G1a	30.402	30.315	28.305	30.344	30.588	3.851
G2a	30.076	29.824	28.141	30.065	30.412	2.401
G3a	30.474	30.415	28.652	30.391	30.533	3.283
G4a	30.221	30.024	28.412	30.172	30.407	2.37
G5a	29.816	29.592	28.127	29.818	30.304	1.875
G6a	29.631	29.373	28.026	29.671	30.267	1.73
G7a	29.758	29.66	28.319	29.791	30.253	1.676
G8a	29.179	28.978	28.182	29.248	29.915	0.844
G9a	29.762	29.532	28.357	29.804	30.175	1.424
G10a	29.908	29.711	28.096	29.859	30.37	2.177
J1a	30.329	30.209	28.037	30.284	30.634	4.464
J2a	30.187	30.037	28.254	30.15	30.46	2.701
J3a	29.745	29.542	27.804	29.83	30.467	2.753
J4a	29.999	29.784	28.01	30	30.456	2.68
J5a	29.92	29.686	27.906	29.922	30.501	3.01
J6a	29.966	29.876	28.544	29.965	30.219	1.562
J7a	29.895	29.851	28.332	29.874	30.316	1.922
SL1a	30.197	30.184	28.600	30.172	30.398	2.325
WL1a	29.024	28.891	27.817	28.892	29.954	0.912
WL2a	29.752	29.695	28.077	29.807	30.378	2.217
CY1a	31.110	31.111	28.545	30.798	30.856	12.907
CY2a	31.370	31.370	28.455	30.882	30.918	23.331
CY3a	30.854	30.850	28.003	30.689	30.815	9.832
CY4a	31.104	31.089	28.336	30.872	30.911	21.445

Appendix 4. Climate information calculated as annual averages for four year previous of March 2014.

Station	Daily Precipitation Average	Mean Annual Precipitation	Daily Evaporation Average	Mean Annual Evaporation	Mean Annual P-E	Annual VPD	Annual RHmax
BL1a	5.435797399	1985.425	4.083367556	1491.45	493.975	0.700443	58.88597
CY1a	3.203422313	1170.05	5.713073238	2086.7	-916.65	1.198382	52.15934
CY2a	4.753661875	1736.275	5.130869268	1874.05	-137.775	0.928823	60.46605
CY3a	2.874058864	1049.75	5.412457221	1976.9	-927.15	1.16675	51.84052
CY4a	5.327104723	1945.725	6.20971937	2268.1	-322.375	1.426563	48.16023
G1a	3.731827515	1363.05	4.306639288	1573	-209.95	0.805349	53.02177
G2a	3.769815195	1376.925	4.366735113	1594.95	-218.025	0.81728	53.28816
G3a	3.710130048	1355.125	4.343874059	1586.6	-231.475	0.811732	53.69144
G4a	4.34072553	1585.45	4.365229295	1594.4	-8.95	0.793601	54.98713
G5a	4.122861054	1505.875	4.300752909	1570.85	-64.975	0.769852	55.09665
G6a	6.044695414	2207.825	4.149623546	1515.65	692.175	0.80391	54.18775
G7a	6.121013005	2235.7	4.051334702	1479.75	755.95	0.784874	54.04038
G8a	5.854620123	2138.4	3.799178645	1387.65	750.75	0.677261	56.86372
G9a	4.594729637	1678.225	4.260232717	1556.05	122.175	0.86797	51.23073
G10a	4.44715948	1624.325	4.351403149	1589.35	34.975	0.839548	54.25743
J1a	3.168309377	1157.225	4.348528405	1588.3	-431.075	0.847714	51.38754
J2a	3.045790554	1112.475	4.321423682	1578.4	-465.925	0.856751	50.22218
J3a	3.291170431	1202.1	4.333196441	1582.7	-380.6	0.841092	51.32389
J4a	5.837166324	2132.025	4.199315537	1533.8	598.225	0.82594	53.5089
J5a	4.942642026	1805.3	4.258042437	1555.25	250.05	0.790671	56.19774
J6a	5.57652293	2036.825	4.242984257	1549.75	487.075	0.773408	57.04524
J7a	5.418959617	1979.275	4.210540726	1537.9	441.375	0.775492	56.30767
SL1a	5.435797399	1985.425	4.083367556	1491.45	493.975	0.700443	58.88597
WL1a	5.274195756	1926.4	4.158932238	1519.05	407.35	0.72604	58.46201
WL2a	5.274195756	1926.4	4.158932238	1519.05	407.35	0.72604	58.46201

Appendix 5. Climate information calculated as winter/spring average for four years previous of March 2014.

Station	Daily Winter/spring Precipitation	Mean Winter/spring precipitation	Daily Winter/spring Evaporation	Mean Winter/spring Evaporation	Mean Winter/spring P-E	VPD	RHmax
BL1a	3.436338798	628.85	3.723224044	681.35	-52.5	0.672762	56.15546
CY1a	0.646174863	118.25	6.13442623	1122.6	-1004.35	1.320899	46.67869
CY2a	1.059289617	193.85	5.309562842	971.65	-777.8	0.993516	56.92322
CY3a	0.819535519	149.975	5.706284153	1044.25	-894.275	1.306335	45.88279
CY4a	1.011202186	185.05	6.842622951	1252.2	-1067.15	1.700302	39.77951
G1a	2.15273224	393.95	3.901912568	714.05	-320.1	0.773928	49.6597
G2a	2.183060109	399.5	3.947540984	722.4	-322.9	0.784568	49.93907
G3a	2.152459016	393.9	3.931693989	719.5	-325.6	0.779794	50.35888
G4a	2.482650273	454.325	3.953278689	723.45	-269.125	0.760082	51.83019
G5a	2.307240437	422.225	3.894808743	712.75	-290.525	0.739013	51.88675
G6a	2.885382514	528.025	3.768032787	689.55	-161.525	0.779053	50.7873
G7a	2.716803279	497.175	3.679234973	673.3	-176.125	0.768921	50.43128
G8a	2.479644809	453.775	3.461748634	633.5	-179.725	0.669781	53.28292
G9a	2.030601093	371.6	3.860382514	706.45	-334.85	0.841758	47.66311
G10a	2.41079235	441.175	3.948087432	722.5	-281.325	0.802356	51.10423
J1a	1.919535519	351.275	3.944262295	721.8	-370.525	0.814401	47.99891
J2a	1.858060109	340.025	3.925136612	718.3	-378.275	0.820949	46.82391
J3a	2.041120219	373.525	3.928961749	719	-345.475	0.807101	47.9168
J4a	2.717486339	497.3	3.806010929	696.5	-199.2	0.801134	50.01544
J5a	2.256830601	413	3.86557377	707.4	-294.4	0.760134	53.03552
J6a	2.708469945	495.65	3.853005464	705.1	-209.45	0.744419	53.80574
J7a	2.72773224	499.175	3.822677596	699.55	-200.375	0.74251	53.13115
SL1a	3.436338798	628.85	3.723224044	681.35	-52.5	0.672762	56.15546
WL1a	3.406147541	623.325	3.785519126	692.75	-69.425	0.694044	55.81831
WL2a	3.406147541	623.325	3.785519126	692.75	-69.425	0.694044	55.81831